

# Tooth wear and dentoalveolar remodeling are key factors of morphological variation in the Dmanisi mandibles

Ann Margvelashvili<sup>a,b,1</sup>, Christoph P. E. Zollikofer<sup>a</sup>, David Lordkipanidze<sup>b,1</sup>, Timo Peltomäki<sup>c</sup>, and Marcia S. Ponce de León<sup>a</sup>

<sup>a</sup>Anthropological Institute and Museum, University of Zurich, CH-8057 Zurich, Switzerland; <sup>b</sup>Georgian National Museum, 0105 Tbilisi, Georgia; and <sup>c</sup>Oral and Maxillofacial Unit, Department of Ear and Oral Diseases, Tampere University Hospital and Department of Otolaryngology, Tampere University, FI-33521 Tampere, Finland

Contributed by David Lordkipanidze, September 2, 2013 (sent for review May 25, 2013)

**The Plio-Pleistocene hominin sample from Dmanisi (Georgia), dated to 1.77 million years ago, is unique in offering detailed insights into patterns of morphological variation within a paleodeme of early *Homo*. Cranial and dentoalveolar morphologies exhibit a high degree of diversity, but the causes of variation are still relatively unexplored. Here we show that wear-related dentoalveolar remodeling is one of the principal mechanisms causing mandibular shape variation in fossil *Homo* and in modern human hunter-gatherer populations. We identify a consistent pattern of mandibular morphological alteration, suggesting that dental wear and compensatory remodeling mechanisms remained fairly constant throughout the evolution of the genus *Homo*. With increasing occlusal and interproximal tooth wear, the teeth continue to erupt, the posterior dentition tends to drift in a mesial direction, and the front teeth become more upright. The resulting changes in dentognathic size and shape are substantial and need to be taken into account in comparative taxonomic analyses of isolated hominin mandibles. Our data further show that excessive tooth wear eventually leads to a breakdown of the normal remodeling mechanisms, resulting in dentognathic pathologies, tooth loss, and loss of masticatory function. Complete breakdown of dentognathic homeostasis, however, is unlikely to have limited the life span of early *Homo* because this effect was likely mediated by the preparation of soft foods.**

aging | compensatory mechanisms | toothpick | local periodontitis | early Pleistocene *Homo*

**A**lthough patterns of dental micro- and macrowear and wear-related pathologies are amply documented in the hominin fossil record (1–5), processes of in vivo dentoalveolar remodeling (3, 6, 7) and their potential influence on dentognathic morphology are only beginning to be studied in fossil hominins (8). In modern human hunter-gatherer populations, remodeling of dentoalveolar hard tissue is triggered mainly by dental wear, aging, pathologies, and trauma. Wear-related remodeling can be understood as a mechanism of in vivo modification that maintains masticatory function (3, 7, 9–14). Three main processes are typically identified (Fig. 1):

- i) Wear-induced reduction of dental crown height leads to alterations in masticatory biomechanics. This triggers alveolar bone remodeling, yielding dislocation of dental structures and eventual continuous eruption of all teeth. As an effect, occlusal contact between upper and lower teeth is maintained (15–17), and the position and orientation of the occlusal plane relative to the temporomandibular joints (TMJs) is held approximately constant, thus preventing the “wear-out” (18) of the TMJs.
- ii) The reduction of mesiodistal crown dimensions through interproximal dental wear triggers alveolar bone remodeling in the mesiodistal direction. This leads to mesial drift of the post-canine dentition and shortening of the dental arcade (19).

- iii) In the anterior dentition, remodeling induced by interproximal wear results in increased lingual tipping; that is, teeth become more upright relative to the alveolar plane (7).

As an effect of mesial drift, interproximal contacts between adjacent postcanine teeth are preserved. Similarly, as an effect of lingual tipping, interproximal contacts between incisors are preserved. During an individual's lifetime, the combined, accumulated effects of continuous eruption, mesial drift, and lingual tipping tend to result in an edge-to-edge bite in the front dentition (7) and in significant changes in mandibular morphology (13, 20).

The site of Dmanisi, Georgia, has yielded a crucial sample of early Pleistocene hominin fossils along with a rich vertebrate fauna and mode I (Oldowan) lithic implements (21, 22). Site occupation began shortly after 1.85 Ma (million years ago) (23); the fossils are dated to 1.77 Ma (21, 23–26). The Dmanisi hominin sample comprises five individuals that document dentognathic development from adolescence to old age, thus providing a unique opportunity to study wear-related dentognathic variation in a sample that comes from a single point in space and geological time (26–29). Various hypotheses have been proposed to explain the high degree of variation seen in the Dmanisi mandibles, ranging from intrataxon sexual dimorphism to intertaxon

## Significance

**The mandibles of the early Pleistocene hominins from Dmanisi, Georgia, exhibit wide morphological variation, but the causes of diversity remain largely unknown. Here we quantify the effects of heavy tooth wear and wear-related bone remodeling on mandibular variation. Using modern hunter-gatherer populations as a reference, we show that features such as dental arcade form, mandibular corpus height, and symphyseal inclination change substantially with progressive tooth wear. These data indicate that the Dmanisi mandibles reflect normal within-population variation augmented by interindividual differences in wear-related bone remodeling. Dmanisi further provides the first clear evidence for toothpick-induced local periodontitis. This study illustrates how excessive tooth wear leads to dentognathic pathology and complete tooth loss, which was evidently compensated for by culturally mediated food processing.**

Author contributions: A.M., C.P.E.Z., D.L., T.P., and M.S.P.d.L. designed research; A.M., C.P.E.Z., and M.S.P.d.L. performed research; A.M., C.P.E.Z., and M.S.P.d.L. contributed new reagents/analytic tools; A.M., C.P.E.Z., D.L., and M.S.P.d.L. analyzed data; and A.M., C.P.E.Z., and M.S.P.d.L. wrote the paper.

The authors declare no conflict of interest.

<sup>1</sup>To whom correspondence may be addressed. E-mail: dlordkipanidze@museum.ge or margvelashvili@aim.uzh.ch.

This article contains supporting information online at [www.pnas.org/lookup/suppl/doi:10.1073/pnas.1316052110/-DCSupplemental](http://www.pnas.org/lookup/suppl/doi:10.1073/pnas.1316052110/-DCSupplemental).

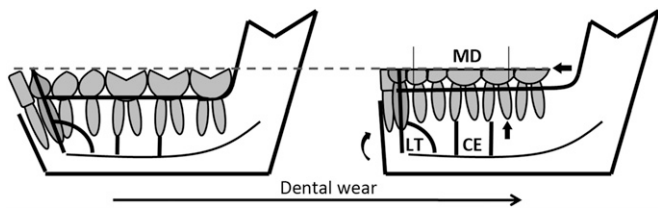


**Fig. 1.** Mechanisms of in vivo dentoalveolar remodeling. Continuous eruption (CE) is tracked by the distance between the mandibular canal and root apices. Mesial drift (MD) is tracked by the length of the posterior dental arcade from M2 to P3. Lingual tipping (LT) is tracked by the angle of inclination of the anterior teeth (incisors and canines) relative to the mandibular canal.

variation (25, 27–31). Here we focus on in vivo dentognathic remodeling as a potential mechanism contributing to the remarkable dentognathic variation in Dmanisi and differentiate normal remodeling processes from pathologic alterations. Using direct observations and data derived from computed tomography (CT) and scanning electron microscopy (SEM), we quantify dental wear (DW), continuous eruption (CE), mesial drift (MD), and lingual tipping (LT) in the following groups: the Dmanisi mandibles [specimens D2735, D211, D2600, D3900 (Fig. 2 and Fig. S1) and KNM-WT 15000 (grouped as early Pleistocene *Homo*)];

the middle Pleistocene mandibles from Tighenif ( $n = 3$ ) and Atapuerca Sima de los Huesos (SH) ( $n = 4$ ); and mandibles of modern hunter–gatherer populations from Australia ( $n = 26$ ) and Greenland ( $n = 15$ ) (Table S1), which all show substantial intragroup variation in dental wear. Measurement protocols are specified in *Materials and Methods* and in Table S2; abbreviations are listed in Table S3. It is well known that dental wear rates (amount of wear per year of life) vary substantially between populations as an effect of differences in food properties (e.g., abrasiveness) and paramasticatory tooth use (32, 33). To permit comparisons between different populations, remodeling rates are thus calculated per wear stage.

### Results and Discussion

The Dmanisi mandibles compose a wide spectrum of wear-related dentognathic variation from moderate overall wear in the subadult D2735 and young adult D211 individuals to wear-induced pathological changes in the old adult individual D2600 and edentulousness in the senile individual D3900.

Mandible D2735 is associated with the subadult cranium D2700 (27, 34). The socket of the right third molar (RM3) contained a tooth bud, which was found in isolation. The left side bears no evidence of an M3 socket, possibly indicating LM3 agenesis (see refs. 35 and 36 for similar cases). Although the second molars (M2) exhibit moderate occlusal wear, the first molars

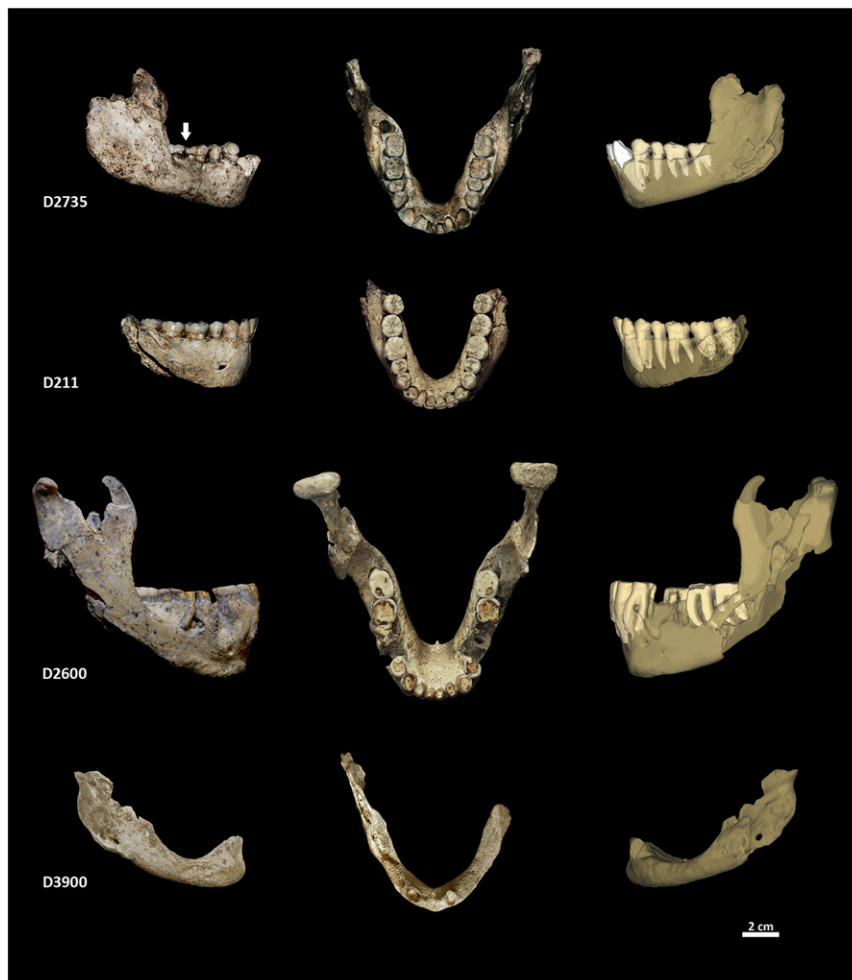


**Fig. 2.** Dmanisi mandibles. Right lateral and occlusal views are photographs taken from original specimens; left lateral views are CT-based 3D reconstructions highlighting internal structures. The canines and incisors of D2735 were found in isolation and digitally reinserted into their sockets. Arrow indicates toothpick lesion.

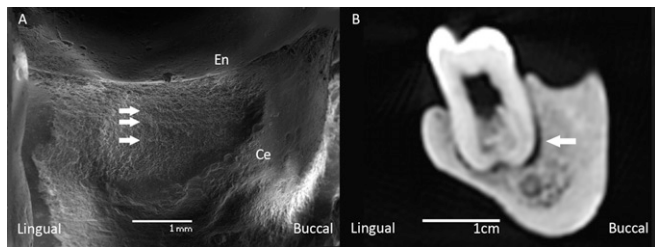


**Fig. 3.** D2735 toothpick lesion. (A) Parallel horizontal scratches on the disto-buccal surface of the RM1. (B) CT cross-section at the level of RM2: arrow indicates local marginal periodontitis. En, enamel; Ce, cementum.

(M1) show substantial occlusal wear with dentine exposure and slight tertiary dentine formation (37)\* in the distal portion of the occlusal surface at the exposed areas of the teeth. The disto-buccal cervical area of the RM1 exhibits a half-cylinder-shaped interproximal wear groove (Fig. 2 and Fig. S1). A similarly shaped opposing groove is present on the mesio-lingual cervical area of RM2, indicating the repeated use of a “toothpick” (38, 39). SEM of the RM1 groove reveals parallel horizontal scratches (Fig. 3A), likely resulting from toothpick-induced mechanical abrasion (38, 39). A marked gap exists between the mesial root of the RM2 and the surrounding alveolar bone (Fig. 3B). Because this is the only gap between a tooth root and its alveolar socket, it likely indicates a local marginal periodontitis related to the toothpick use. The molar and premolar (P) root apices are within 5 mm of the mandibular canal, and the length of the dental arcade from M2 to P3 is 44.0 mm. The anterior dentition is strikingly procumbent. Moderate linear enamel hypoplasia (LEH) is found on the cervical thirds of the crowns of LM2, P4s, P3s, canines, and lateral incisors. The distal corners and incisal edges of the lateral incisors bear evidence of *in vivo* chipping of the enamel, which is indicative of heavy masticatory and/or paramasticatory loads (40). Mandible D211, which is likely associated with cranium D2282 (27, 29), represents a young adult with higher overall wear than D2735. The dental arcade between M2 and P3 is 42.3 mm long. The anterior dentition is less procumbent than in D2735 (Fig. 4). The RM3 is tipped lingually, and there is mild dental crowding in the area of the canines and second incisors. The canines show light LEH in the cervical region of their crowns. The distal corner of LI2 shows *in vivo* enamel chipping, possibly indicating paramasticatory activity. All teeth of the adult mandible D2600 exhibit advanced stages of wear. The M2s, RM1, and incisors (Is) are all worn down to the cemento-enamel junction. Extensive tertiary dentine formation and even pulp-chamber exposure can be observed on the M2s, RM1, canines (Cs), and all four Is. The molar and premolar root apices are located higher above the mandibular canal than in D2735 and D211. The length of the dental arcade is 44.2 mm. The front teeth are significantly less procumbent than in D211 and D2735 (Fig. 4C). The alveolar bone around the roots of RM1 and RI2 bears evidence of periapical cyst formation (Fig. S2A and B). LM1 was lost perimortem; the P4s are not preserved, but partial resorption of their alveolar sockets indicates tooth loss before death. The third premolars (P3s) are tilted distally, which is characteristic for teeth adjacent to edentulous areas. The P3s, Cs, and Is show marked cementum hyperplasia around the roots (Fig. S2C), which—together with heavy occlusal wear and labial rounding of the occlusal surface of the Is—is indicative of extensive use of the front dentition in paramasticatory activities

\*Following the definitions of ref. 37, primary dentine is deposited during tooth formation; secondary dentine is formed continuously, past dental eruption and into adulthood; and tertiary (or reparative) dentine is formed as a reaction to dental injury.

(41–44). The external symphyseal surface below the incisor roots shows evidence of bone resorption resulting in a notable infra-dental depression and a chin-like morphology of the symphysis (Fig. 2). Mandible D3900, which is associated with the edentulous cranium D3444 (28), represents an elderly individual. Its alveolar process is almost completely atrophied, indicating massive tooth loss several years antemortem (28, 45). The only tooth still in place pre-mortem (but lost post-mortem) was the left canine (Fig. 2). This is evidenced by its alveolar socket, which had not yet undergone notable bone remodeling (28, 45) but exhibits marked lingual tipping (Fig. 4C). A chin-like eminence similar to that of D2600 is present here as well.

Fig. 4 and Figs. S3 and S4 document continuous eruption (CE-M2, CE-M1, CE-P4), mesial drift (MD), and lingual tipping (LT-C, LT-I2, LT-I1) as a function of dental wear (DW). Size-standardized measurements of relative continuous eruption (rCE-M1) and relative mesial drift (rMD), as well as LT-C exhibit significant correlation with DW (Tables S4 and S5), revealing a common pattern of wear-related dentoalveolar remodeling and associated mandibular shape change in all groups (Fig. 4 and Figs. S3 and S4). With increasing occlusal and interproximal wear, rCE and LT increase, whereas rMD decreases. Within each group, morphological differences between mandibles exhibiting light versus heavy dental wear are substantial. Group-specific regression of rCE-M1, rMD, and LT-C on DW yields estimates of morphological change in an average-sized mandible [mandibular size (MS) = 22] between wear stages 1 and 8 (or 9 if applicable). CE at M1 increases by 12.5 mm in Dmanisi/early Pleistocene *Homo*, by 8.6 mm in Australians, and by 7.4 mm in Greenlanders. MD results in a reduction of dental arcade length by 9.3 mm (20%) in Dmanisi/early Pleistocene *Homo*, by 5.7 mm in Australians (15%), and by 4.2 mm (12%) in Greenlanders (Fig. 4A and B; Fig. S3A and B). The LT angle at Cs decreases by 34° in the Dmanisi sample, 58° in the Tighenif sample, 16° in the Atapuerca SH sample, and 13–14° in the modern human population samples (Fig. 4C and Fig. S3C). In keeping with continuous eruption of the dentition, mandibular corpus height at M1 and P4, as well as symphysis height, tend to increase until DW stage 7 (early Pleistocene *Homo*: 6.5 mm/10 mm; *Homo sapiens*: 5 mm/4.4 mm) (Fig. 4D; Fig. S5A and B). Later on, corpus and symphysis heights decrease as an effect of incipient bone resorption around the alveolar borders.

Regressions of rCE-M1, rMD, and LT-C on DW also provide estimates of remodeling rates as a function of dental wear (Fig. S3). Resampling analysis (*Materials and Methods*) shows that rates of wear-related rCE-M1 and LT-C are more substantial in Dmanisi and early Pleistocene *Homo* than in modern *H. sapiens*, whereas rates of rMD are similar in all groups. Greenlanders differ from all other groups in a low position of the mandibular canal, resulting in large overall distances between this structure and root apices. With regard to Dmanisi, our data thus provide support for the hypothesis that mandibular shape variation in this sample represents the normal range of variation expected in a single paleopopulation comprising individuals with light-to-heavy dental wear.

To interpret commonalities and differences between groups, we have to consider four main factors influencing dental wear and bone remodeling processes: (i) bite pressure (force exerted per dental crown area unit); (ii) bite force direction (which depends on the directionality of muscle action); (iii) the physiology of the periodontal ligament, which holds the teeth in their sockets and mediates dentoalveolar remodeling; and (iv) abrasiveness of the food. Early Pleistocene *Homo* has higher rCE-M1 rates than modern humans (Fig. 4A and Fig. S3A), which signifies that there is more eruption per amount of dental wear in the former compared with the latter group. Because rCE-M1 rates are measured relative to dental wear grade, differences in food abrasiveness are unlikely to explain this pattern. It appears more

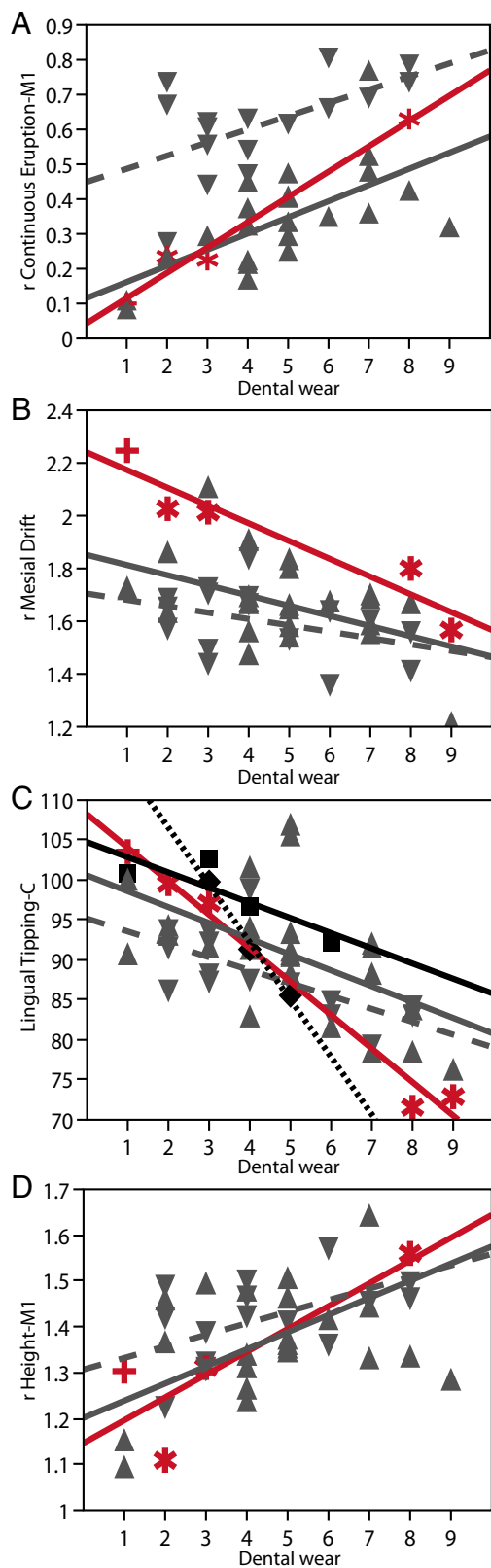


**Fig. 4.** Wear-related dentoalveolar remodeling in fossil *Homo* and modern humans. (A) Relative continuous eruption of first molars (mean of L and R). (B) Relative mesial drift (rMD). (C) Lingual tipping of canines. (D) Relative corpus height at M1. Red symbols and regression lines: Dmanisi [stars, from left to right: D2735 (DW2), D211 (DW3), D2600 (DW8), D3900 (DW9)] and KNM-WT15000 (plus sign); black diamonds and black-stippled line, Tighenif; black squares and solid line, Atapuerca SH; gray symbols and lines, *H. sapiens*

probable that higher masticatory loads (bite pressure) in the fossil sample elicited a higher rate of remodeling. Alternatively, rate differences may reflect differences in group-specific tooth crown height.

Masticatory muscles exert a strong distomesially directed force component on the dental arcade (46), which is the major cause of interproximal tooth wear and subsequent relocation of the posterior dentition in the mesial direction (47). Our data indicate that rates of rMD were similar in early Pleistocene *Homo* and the modern human hunter-gatherer populations analyzed here (Fig. 4B and Fig. S3B), thus providing support for the hypothesis that mesiodistal forces and masticatory biomechanics were largely similar in these groups (48).

Group-specific differences in rates of LT-C (Fig. 4C and Fig. S3C) may reflect differences in anterior dentognathic morphology and/or bite-force patterns. Young adults of early Pleistocene *Homo* tended to have more procumbent front teeth than their modern human peers, such that the amount of lingual tipping resulting from interproximal wear between the front teeth likely was greater than in the orthognathic morphology characteristic of modern humans (8). Also, bite-force patterns in the anterior dentition might have differed between groups, e.g., due to different paramasticatory activities. However, because all populations considered here bear evidence of paramasticatory use of the front dentition (Dmanisi, Atapuerca SH, Australians, and Greenlanders), we consider this hypothesis less likely. Overall, we infer that wear-related rates of dentoalveolar remodeling are mostly influenced by taxon-specific mandibular morphology and masticatory loads.

Having established the typical pattern of wear-related dentoalveolar remodeling, it is possible to identify a series of dentognathic pathologies that result from excessive tooth wear and eventually lead to a breakdown of the normal compensatory remodeling mechanisms. In the D2600 mandible, complete or nearly complete wear of the crowns of M2s, RM1, Cs, and all four incisors led to massive dentine and even pulp-chamber exposure. This entailed chronic root canal infection, periapical cyst formation, and resorption of the affected periapical bone around RM1 and RI1. Hypercementosis (increased cementum thickness) around the roots of the anterior teeth (Fig. S2C) indicates high masticatory/paramasticatory loads (44) and advanced age (49). Ensuing calcification and overload of the periodontal ligament (50) might have led to loss of periodontal hafting, which then caused the marked lingual “overtipping” of the incisors, concomitant root exposure on the labial side, and incipient resorption on the external bony plate of the symphysis. Mandible D3900 illustrates the final stage of the breakdown sequence: loss of all teeth (except one canine) followed by complete/partial resorption of the posterior/anterior alveolar process.

The pattern of tooth loss and alveolar bone resorption in D2600 and D3900 is similar to the breakdown sequence reported in modern humans (15, 51) and Neanderthals (52), indicating similar mechanisms of dentognathic failure in Pleistocene *Homo* and modern humans. The alveolar bone resorption pattern of D3444/D3900 indicates that this individual survived without functional teeth for several years (28, 45). This suggests that behavioral compensatory strategies such as tool-mediated preparation of soft food might have played a crucial role in extending the life expectancy of hominins beyond the functional lifetime of the dentognathic system. The breakdown sequence described here thus likely represents a shared pattern of dentognathic wear-out in hominins, hominoids (53, 54), and even some nonanthropoid primates, such as ring-tailed lemurs (55). Culturally mediated food

Australia (normal triangles and solid line) and Greenland (inverted triangles and dashed line). Regression statistics are summarized in Table S4.

processing as a behavioral compensatory mechanism after complete breakdown, however, seems to be a unique hominin feature.

Dmanisi mandible D2735 adds to the growing evidence for habitual use of toothpicks in early Pleistocene *Homo* at 1.8 Ma (39). Although there is ample evidence for toothpicking in mid-to-late Pleistocene hominins (39), D2735 shows a direct link between regular dental grooming and dentognathic pathology. Toothpicking in this individual likely served to remove nutritional leftovers, but it caused visible damage to the dental cervix and the interdental alveolar crest and resulted in a gap between the M2 mesial root and its alveolar socket, which is characteristic of local marginal periodontitis (56).

Mandibular morphology is often used for hominin taxonomy (57–62), not least because mandibles are typically better preserved and more numerous than crania or other skeletal parts. However, it is also known that mandibles are notoriously variable, which led to the often-cited saying that “while the skull is the creation of God, the jaw is the work of the Devil” (ref. 63, p. 353). Our study demonstrates that wear-induced dentoalveolar remodeling contributes substantially to mandibular shape variation within hominin taxa. Differences between fossil hominin mandibles in dental crown dimensions, crown shape (mesio-distal to bucco-lingual width), corpus height, symphyseal height, symphyseal inclination, and prognathism thus need to be analyzed in the context of wear-related *in vivo* modifications before taxonomic implications are drawn. Specifically, Dmanisi shows that wear-related remodeling greatly affects the morphology of the dental arcade, whose procumbent and parabolic shape becomes anteroposteriorly short and squared-off, resulting in a relatively more protruding chin region.

Dentoalveolar remodeling also plays a significant role in assessing taxonomic diversity in early *Homo*. In a comparative analysis of recent finds from Koobi Fora (64), mandible KNM-ER 60000 was associated taxonomically with maxilla KNM-ER 62000 and cranium KNM-ER 1470 based on their matching orthognathic profiles. Mandible KNM-ER 1802, which exhibits pronounced alveolar prognathism, was attributed to a different taxon. This latter specimen represents a young adult, exhibiting only light dental wear (DW stage 1) and a procumbent front dentition (as indicated by the preserved root fragments). KNM-ER 60000, which is similar in overall dentognathic dimensions to D2600, has a heavily worn dentition (DW stage 5) and exhibits marked lingual tipping (supporting information p. 18 in ref. 64), which results in a comparatively orthognathic morphology (Fig. S6). Differences between the two mandibles may thus be largely due to different degrees of dentoalveolar remodeling. Further research is required to quantify age- and wear-related dentognathic changes in an extended sample of fossil and extant taxa and to assess the impact of dentoalveolar remodeling processes on patterns of intra-versus intertaxon dentognathic variation in fossil hominins.

## Materials and Methods

The sample comprises mandibles D2735, D211, D2600, and D3900 from Dmanisi (Georgia), a sample of early-to-mid Pleistocene *Homo* mandibles from Eurasia and Africa ( $n = 8$ ; Table S1) [KNM-WT 15000, Tighenif (T2, T3, T1) (65), Atapuerca (AT-607, AT-300, AT-605, AT-888) (58, 66)], a modern human sample of Australian aborigines ( $n = 26$ ) from the Duckworth Collection, Leverhulme Centre for Human Evolutionary Studies, and an Inuit sample ( $n = 15$ ) from the collections of the Anthropological Institute and Museum of the University of Zurich. DW was scored using the Molnar scale

(67) extended by an additional grade 9 for extreme wear (two or fewer heavily worn teeth *in situ*). Within populations, DW is typically correlated with chronological age (32). However, considerable differences exist between populations in DW rates, such that DW cannot be used as a proxy for chronological age in cross-population comparisons. Tomographic data were acquired with multislice helical CT in axial and coronal orientations (0.625-mm collimation, pitch 0.75). Cross-sectional images (512 × 512 pixels) were reconstructed at 0.1- to 0.2-mm isotropic voxel volumes. The CT data volumes were transferred to a high-performance graphics workstation. Measurements of CE, MD, LT, and overall mandibular dimensions were taken with the software VGStudioMax 20 ([www.volumegraphics.com/](http://www.volumegraphics.com/)) (see Table S2 for details). Where available, all measurements were taken from CT data acquired from the original specimens. Otherwise CTs of casts were used, or data were collected from the literature (details are given in Table S1).

Linear and angular measurements of dentoalveolar remodeling were taken with reference to the mandibular canal, as this structure remains stable during growth and aging (68, 69). Continuous eruption of M2, M1, and P4 (CE-M2, CE-M1, CE-P4) was measured by the distance between the mesial root apex to the bottom of the mandibular canal (modified from ref. 13). As a proxy of MD, posterior dental arcade length was measured by the linear distance at the level of the anatomical cervixes between the distal-most point of the M2 to the mesial-most point of the P3. Lingual tipping of Cs and Is (LT-C, LT-I2, and LT-I1) was measured by the angle between the main axis of the tooth (or tooth socket, if the tooth was not present) and a plane parallel to the mandibular canals. MS was quantified by the geometric mean of three linear distances: symphyseal thickness, bilateral mental foramen breadth, and height of the mental foramen above the base of the mandibular corpus. MS does not correlate with DW (Fig. S7) and was thus used to calculate size-standardized measurements of CE ( $rCE = CE/MS$ ) and MD ( $rMD = MD/MS$ ). Measurement definitions for corpus height at P4 and M1 and for symphyseal height are from Wood (70): minimum distance between the most inferior point on the base of the mandible and the lingual alveolar margin at the midpoints of P4/M1 and at infradentale. Measurements of LT-C for Tighenif and Atapuerca were derived from published photographs and casts (original data of these specimens were not available). SEM imaging of the cervical dental surfaces of the D2735 specimen was performed as follows: a primary mold was taken from the original specimen with the low-viscosity material Optosil-Xantopren VL plus (Heraeus Kulzer). Casts were produced with Crystal Clear (Smooth-On), coated with 16 nm of platinum and examined at different magnifications (1 mm, 500  $\mu$ m, 200  $\mu$ m) in the JEOL SEM.

Statistical analyses were performed with JMP ([www.jmp.com](http://www.jmp.com)) and MATLAB ([www.mathworks.com](http://www.mathworks.com)). Because fossil sample sizes are small, we used resampling statistics to compare group-specific dentoalveolar remodeling rates (= regression slopes of  $rCE$ -M1,  $rMD$ , and  $LT-C$  on DW). Specifically, we compared rates in the Dmanisi + KNM-WT15000 group with rates in modern human populations. To this end, resampling with replacement was used to draw  $K = 80$  random samples of  $n = 9$  *Homo sapiens* specimens, in which each DW score class was represented by one specimen (thus mimicking the DW distribution in the Dmanisi sample). Differences between Dmanisi and *H. sapiens* in sample mean and regression slope were considered statistically significant if the Dmanisi parameters were below the fifth or above the 95th percentile of the empirical distributions evaluated for *H. sapiens*.

**ACKNOWLEDGMENTS.** We thank Marta Mirazón Lahr and Robert A. Foley for providing access to the Australian sample at Leverhulme Centre for Human Evolutionary Studies and Fabio Lahr for help during scanning; Grigol Nemsadze for performing the Dmanisi CT scans at the University Hospital of Tbilisi; Gery Barmettler (University of Zurich) for help with SEM imaging; the late Guram Bumbiashvili (Georgian National Museum) for the photographic documentation of the Dmanisi mandibles; Naoki Morimoto (University of Zurich) for substantial MATLAB input; Jukka Jernvall for a decisive initial discussion; and the reviewers for critical input. This work was supported by the Wenner-Gren Foundation, the A. H. Schultz Foundation, the Swiss National Science Foundation [Scientific co-operation between Eastern Europe and Switzerland (SCOPES) program], and the Shota Rustaveli National Science Foundation.

1. Kaifu Y (2000) Was extensive tooth wear normal in our ancestors? *Anthropol Sci* 108(4):371–385.
2. Scott RS, et al. (2005) Dental microwear texture analysis shows within-species diet variability in fossil hominins. *Nature* 436(7051):693–695.
3. d’Incau E, Couture C, Maureille B (2012) Human tooth wear in the past and the present: Tribological mechanisms, scoring systems, dental and skeletal compensations. *Arch Oral Biol* 57(3):214–229.
4. Scott RS, Teaford MF, Ungar PS (2012) Dental microwear texture and anthropoid diets. *Am J Phys Anthropol* 147(4):551–579.
5. Lucas PW, et al. (2013) Mechanisms and causes of wear in tooth enamel: Implications for hominin diets. *J R Soc Interface* 10(80):20120923.
6. Kaifu Y (2000) Tooth wear and compensatory modification of the anterior dentoalveolar complex in humans. *Am J Phys Anthropol* 111(3):369–392.
7. Kaifu Y, Kasai K, Townsend GC, Richards LC (2003) Tooth wear and the “design” of the human dentition: A perspective from evolutionary medicine. *Am J Phys Anthropol* (Suppl 37):47–61.
8. Ungar PS, Fennell KJ, Gordon K, Trinkaus E (1997) Neandertal incisor beveling. *J Hum Evol* 32(5):407–421.

9. Begg P (1954) Stone age man's dentition. *Am J Orthod* 40(4):298–312.
10. Forsberg C-M, Eliasson S, Westergren H (1991) Face height and tooth eruption in adults: A 20-year follow-up investigation. *Eur J Orthod* 13(4):249–254.
11. Danenberg PJ, Hirsch RS, Clarke NG, Leppard PI, Richards LC (1991) Continuous tooth eruption in Australian aboriginal skulls. *Am J Phys Anthropol* 85(3):305–312.
12. Kaifu Y (1999) Changes in the pattern of tooth wear from prehistoric to recent periods in Japan. *Am J Phys Anthropol* 109(4):485–499.
13. Harris EF, Shiloah Y (2007) A longitudinal study of continued tooth eruption during adulthood. *Dent Anthropol* 20(1):7–15.
14. Kaidonis JA (2008) Tooth wear: The view of the anthropologist. *Clin Oral Investig* 12(Suppl 1):S21–S26.
15. Clarke NG, Hirsch RS (1991) Tooth dislocation: The relationship with tooth wear and dental abscesses. *Am J Phys Anthropol* 85(3):293–298.
16. Whittaker D (1992) Quantitative studies on age changes in the teeth and surrounding structures in archaeological material: A review. *J R Soc Med* 85(2):97–101.
17. Fleischmannova J, Matalova E, Sharpe PT, Miskel I, Radlanski RJ (2010) Formation of the tooth-bone interface. *J Dent Res* 89(2):108–115.
18. Richards LC, Brown T (1981) Dental attrition and degenerative arthritis of the temporomandibular joint. *J Oral Rehabil* 8(4):293–307.
19. Wolpoff MH (1971) Interstitial wear. *Am J Phys Anthropol* 34(2):205–227.
20. Enlow DH, Harris DB (1964) A study of the postnatal growth of the human mandible. *Am J Orthod* 50(1):25–50.
21. Gabunia L, et al. (2001) Dmanisi and dispersal. *Evol Anthropol* 10(5):158–170.
22. Mgeladze A, et al. (2011) Hominin occupations at the Dmanisi site, Georgia, Southern Caucasus: Raw materials and technical behaviours of Europe's first hominins. *J Hum Evol* 60(5):571–596.
23. Ferring R, et al. (2011) Earliest human occupations at Dmanisi (Georgian Caucasus) dated to 1.85–1.78 Ma. *Proc Natl Acad Sci USA* 108(26):10432–10436.
24. Gabunia L, Vekua A, Lordkipanidze D (2000) The environmental contexts of early human occupation of Georgia (Transcaucasia). *J Hum Evol* 38(6):785–802.
25. Gabunia L, et al. (2000) Earliest Pleistocene hominid cranial remains from Dmanisi, Republic of Georgia: Taxonomy, geological setting, and age. *Science* 288(5468):1019–1025.
26. Lordkipanidze D, et al. (2007) Postcranial evidence from early *Homo* from Dmanisi, Georgia. *Nature* 449(7160):305–310.
27. Rightmire GP, Lordkipanidze D, Vekua A (2006) Anatomical descriptions, comparative studies and evolutionary significance of the hominid skulls from Dmanisi, Republic of Georgia. *J Hum Evol* 50(2):115–141.
28. Lordkipanidze D, et al. (2006) A fourth hominid skull from Dmanisi, Georgia. *Anat Rec A Discov Mol Cell Evol Biol* 288(11):1146–1157.
29. Rightmire GP, Van Arsdale AP, Lordkipanidze D (2008) Variation in the mandibles from Dmanisi, Georgia. *J Hum Evol* 54(6):904–908.
30. Schwartz JH (2000) Taxonomy of the Dmanisi crania. *Science* 289(5476):55–56.
31. Skinner MM, Gordon AD, Collard NJ (2006) Mandibular size and shape variation in the hominins at Dmanisi, Republic of Georgia. *J Hum Evol* 51(1):36–49.
32. Walker PL, Dean G, Shapiro P (1991) Estimating age from tooth wear in archaeological populations. *Advances in Dental Anthropology*, eds Kelley M, Larsen CS (Wiley-Liss, New York), pp 169–178.
33. Rösing FW, Kvaal SI (1998) Dental age in adults: A review of estimation methods. *Dental Anthropology*, eds Alt KW, Rösing FW, Teschler-Nicola M (Springer, Berlin), pp 443–468.
34. Vekua A, et al. (2002) A new skull of early *Homo* from Dmanisi, Georgia. *Science* 297(5578):85–89.
35. Wallace JA (1977) Gingival eruption sequences of permanent teeth in early hominids. *Am J Phys Anthropol* 46(3):483–493.
36. Dean MC, Smith BH (2009) *Growth and Development of the Nariokotome Youth, KNM-WT 15000. The First Humans: Origin and Early Evolution of the Genus Homo* (Springer, Berlin), pp 101–120.
37. Foster BL, Hociti FHJ, Somerman MJ (2013) Tooth root development. *Stem Cells in Craniofacial Development and Regeneration*, eds Huang GT-J, Thesleff I (Wiley-Blackwell, Hoboken, NJ), pp 153–177.
38. Bouchneb L, Maureille B (2004) Interproximal grooves on teeth: Experimental reproduction, SEM analysis and application of the results to observations on Neanderthal lineage. *Bull Mem Soc Anthropol Paris* 16(1–2):37–48.
39. Ungar PS, Grine FE, Teaford MF, Pérez-Pérez A (2001) A review of interproximal wear grooves on fossil hominid teeth with new evidence from Olduvai Gorge. *Arch Oral Biol* 46(4):285–292.
40. Fiorenza L, Benazzi S, Kullmer O (2011) Para-masticatory wear facets and their functional significance in hunter-gatherer maxillary molars. *J Archaeol Sci* 38(9):2182–2189.
41. Hinton RJ (1981) Form and patterning of anterior tooth wear among aboriginal human groups. *Am J Phys Anthropol* 54(4):555–564.
42. Corruccini RS, Jacobi KP, Handler JS, Aufderheide AC (1987) Implications of tooth root hypercementosis in a Barbados slave skeletal collection. *Am J Phys Anthropol* 74(2):179–184.
43. Comuzzie AG, Steele DG (1989) Enlarged occlusal surfaces on first molars due to severe attrition and hypercementosis: Examples from prehistoric coastal populations of Texas. *Am J Phys Anthropol* 78(1):9–15.
44. Pinheiro BC, Pinheiro TN, Capelozza ALA, Consolaro A (2008) A scanning electron microscopic study of hypercementosis. *J Appl Oral Sci* 16(6):380–384.
45. Lordkipanidze D, et al. (2005) Anthropology: The earliest toothless hominid skull. *Nature* 434(7034):717–718.
46. Lucas PW (2004) *Dental Functional Morphology. How Teeth Work* (Cambridge Univ Press, Cambridge, UK; New York), pp 37–39.
47. Osborn JW (1961) An investigation into the interdental forces occurring between the teeth of the same arch during clenching the jaws. *Arch Oral Biol* 5(3–):202–211.
48. O'Connor CF, Franciscus RG, Holton NE (2005) Bite force production capability and efficiency in Neandertals and modern humans. *Am J Phys Anthropol* 127(2):129–151.
49. Consolaro A, Consolaro RB, Francischone LA (2012) Cementum, apical morphology and hypercementosis: A probable adaptive response of the periodontal support tissues and potential orthodontic implications. *Dental Press J Orthod* 17(1):21–30.
50. Shiba H, et al. (2000) Effects of ageing on proliferative ability, and the expressions of secreted protein, acidic and rich in cysteine (SPARC) and osteoprotegerin (osteoclastogenesis inhibitory factor) in cultures of human periodontal ligament cells. *Mech Ageing Dev* 117(1–3):69–77.
51. Marcus SE, Drury TF, Brown LJ, Zion GR (1996) Tooth retention and tooth loss in the permanent dentition of adults: United States, 1988–1991. *J Dent Res* 75(Spec No):684–695.
52. Smith P (1976) Dental pathology in fossil hominids: What did neanderthals do with their teeth? *Curr Anthropol* 17(1):149–151.
53. Schultz AH (1935) Eruption and decay of the permanent teeth in primates. *Am J Phys Anthropol* 19(4):489–581.
54. Miles AEW, Grigson C (2003) *Colyer's Variations and Diseases of the Teeth of Animals* (Cambridge Univ Press, Cambridge, UK; New York).
55. Cuzzo FP, Sauther ML (2006) Severe wear and tooth loss in wild ring-tailed lemurs (*Lemur catta*): A function of feeding ecology, dental structure, and individual life history. *J Hum Evol* 51(5):490–505.
56. Huuomonen S, Ørstavik D (2002) Radiological aspects of apical periodontitis. *Endod Topics* 1:3–25.
57. White TD, Johanson DC (1982) Pliocene hominid mandibles from the Hadar Formation, Ethiopia: 1974–1977 collections. *Am J Phys Anthropol* 57(4):501–544.
58. Rosas A (1995) Seventeen new mandibular specimens from the Atapuerca/Ibeas Middle Pleistocene Hominids sample (1985–1992). *J Hum Evol* 28:533–559.
59. Sherwood RJ, Hlusko LJ, Duren DL, Emch VC, Walker A (2005) Mandibular symphysis of large-bodied hominoids. *Hum Biol* 77(6):735–759.
60. Guy F, et al. (2008) Symphyseal shape variation in extant and fossil hominoids, and the symphysis of *Australopithecus bahrelghazali*. *J Hum Evol* 55(1):37–47.
61. Lague MR, Collard NJ, Richmond BG, Wood BA (2008) Hominid mandibular corpus shape variation and its utility for recognizing species diversity within fossil *Homo*. *J Anat* 213(6):670–685.
62. de Ruiter DJ, et al. (2013) Mandibular remains support taxonomic validity of *Australopithecus sediba*. *Science* 340(6129):1232997.
63. Rak Y (1998) Does any Mousterian cave present evidence of two hominid species? *Neandertals and Modern Humans in Western Asia*, eds Akazawa T, Kenichi A, Bar-Yosef O (Plenum Press, New York), pp 353–365.
64. Leakey MG, et al. (2012) New fossils from Koobi Fora in northern Kenya confirm taxonomic diversity in early *Homo*. *Nature* 488(7410):201–204.
65. Schwartz JH, Tattersall I (2002) *The Human Fossil Record: Craniodental Morphology of Genus Homo (Africa and Asia)* (Wiley-Liss, Hoboken, NJ), Vol 2, pp 296–301.
66. Rosas A (2001) Occurrence of neanderthal features in mandibles from the Atapuerca-SH site. *Am J Phys Anthropol* 114(1):74–91.
67. Molnar S (1971) Human tooth wear, tooth function and cultural variability. *Am J Phys Anthropol* 34(2):175–189.
68. Björk A (1969) Prediction of mandibular growth rotation. *Am J Orthod* 55(6):585–599.
69. Pålsson SR, Kjaer I (2009) Morphology of the mandibular canal and the angulation between the mandibular and mental canals in dry skulls. *Eur J Orthod* 31(1):59–63.
70. Wood B, ed (1991) *Koobi Fora Research Project, Volume 4: Hominid Cranial Remains* (Oxford Univ Press, Oxford), Vol 4, pp 295–296.